Reports

Salt Fingers Observed in the Mediterranean Outflow

Abstract. *Salt fingers, convection cells which constitute a possible mixing mechanism of the ocean, have now been observed in the Mediterranean outflow. The fingers, 6 millimeters in diameter and 24 centimeters long, were photographed below the salinity maximum of the outflow, in an interface 22 centimeters thick where temperature and salinity decreased 0.15°C and 0.03 per mil, respectively.*

Salt fingers consist of descending columns of warm, salty water which exchange heat with interpenetrating, rising columns of cool, less salty water. The index of refraction of the sinking columns is higher than that of the rising columns, permitting the fingers to be photographed. A new instrument named SCIMP, an acronym for Self-Contained Imaging Micro-Profiler, obtained photographs of fingerlike phenomena in the ocean in July 1973, at a strong temperature and salinity step in the Mediterranean outflow. This is the first direct evidence that salt fingers exist in the ocean.

Salt fingers are interesting to oceanographers because they present a possible mechanism for mixing salt and heat downward in the ocean. Munk (*1*) listed the possible vertical mixing processes as mixing along ocean boundaries, by internal waves, by living organisms, or by thermodynamic processes. Woods (*2*) has evidence that mixing occurs in some regions by breaking internal waves. "Salt fingering" is the thermodynamic process applicable to regions where warm, salty water overlies cool, less salty water, as it does in vast areas of the ocean. The system of horizontal, homogeneous layers separated by high-gradient interface regions, which is thought to be generated by salt fingers, is an efficient transport mechanism in theory. Turner (*3*) has shown that vertical transport of salt and heat by the fingers in the interface region is several orders of magnitude greater than expected by molecular diffusion, and that the motion of the rising and sinking columns serves to stir the layers on either side, so that salt and heat are transported efficiently across the layers.

Dense Mediterranean water, both warm and salty, intrudes into the cooler, less salty Atlantic water, forming a salinity maximum at a depth of 1200 m. Beneath this salinity maximum, a staircase profile of layers and interfaces, such as fingers might produce, has been observed (*4*). It was in such a staircase that SCIMP photographed fingers.

The instrument deployed in the outflow produces a collimated beam of laser light 5 cm in diameter which passes horizontally through 160 cm of seawater, then forms an image on a screen of the optical inhomogeneities in its path; this image is a shadowgraph. Objects anywhere along the seawater path are imaged equally well because the light is essentially parallel (*5*). The screen is photographed about once a second as the instrument sinks slowly. In this way, 600 m of the water column can be recorded on 400 feet (122 m) of 16-mm film. Simultaneous measurements of conductivity, temperature, and pressure are made and recorded digitally on tape. The tape record numbers appear on the film, as well as on the tape, for subsequent correlation of the computed temperature and salinity profiles with the images.

The images of salt fingers in the outflow appear in Fig. 1A. The first image, number 20, shows little or no structure because it is above the interface region. The disturbance in the next two frames, 22 and 24, is apparently a transitional stage where some fingers are visible but are in the process of being stirred into the upper layer. Starting one-third of the way down frame 27, continuing on 29, 31, and 33, and finishing one-third of the way down 35, a depth range of 24 cm, there are vertical bands of high contrast which indicate highly organized salt fingers. The remainder of the images show disordered structure in the lower transition region where fingers are being stirred into the lower layer. Well below the interface, the

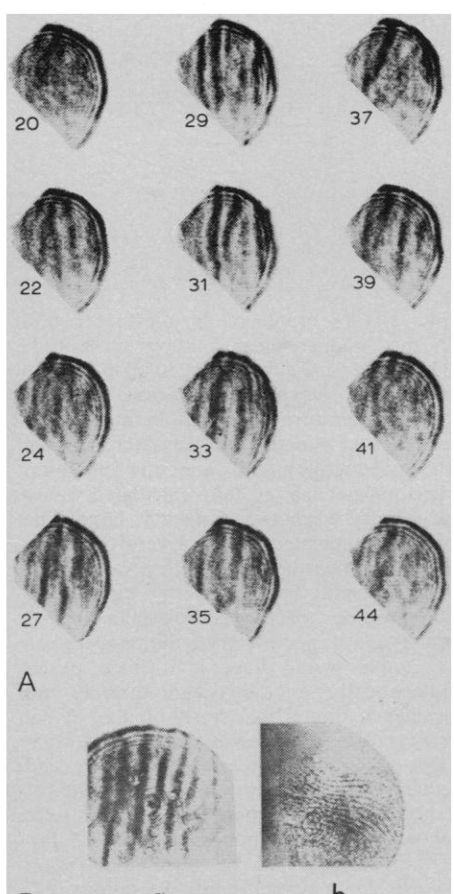

Fig. 1. (A) Shadowgraph images of salt fingers in the Mediterranean outflow. Each image is 5 cm in diameter in the ocean; the vertical separation is proportional to the separation in the ocean. Each number is the last two digits of the record number, which correlates the images to the profile. The dark bands are shadows of descending fingers (high refractive index) and the light bands are shadows of rising fingers (low refractive index). (B) Shadowgraph images in the laboratory tank [reproduced from (*9*)]. Image a shows salt fingers. Image b is a blank pattern after the tank was stirred. The image diameter is 5 cm.

Scoreboard for Reports: In the past few weeks the editors have received an average of 68 Reports per week and have accepted 12 (17 percent). We plan to accept about 12 reports per week for the next several weeks. In the selection of papers to be published we must deal with several factors: the number of good papers submitted, the number of accepted papers that have not yet been published, the balance of subjects, and length of individual papers.

Authors of Reports published in *Science* find that their results receive good attention from an interdisciplinary audience. Most contributors send us excellent papers that meet high scientific standards. We seek to publish papers on a wide range of subjects, but financial limitations restrict the number of Reports published to about 15 per week. Certain fields are overrepresented. In order to achieve better balance of content, the acceptance rate of items dealing with physical science will be greater than average.

images again become structureless (these images are not shown).

Although the shape of the instrument minimizes disturbance of the water, a boundary layer is carried down on the window and mirror through the interface. The erosion of this boundary layer presumably contributes to the optical noise of the measurement. However, interfaces not of the salt fingering type do not show banded structure. Since the optical effects of boundary layer erosion are present for any type of interface encountered, the bands are not a boundary layer effect.

The oceanic images are correlated with the profile in Fig. 2A. The region of high gradient is only about 22 cm thick, but the differences in temperature and salinity across it are 0.15°C and 0.03 per mil, respectively. The destabilizing effect resulting from the salinity difference between the layers is compensated to within 4 $\mu g/cm^3$ by the stabilizing effect resulting from temperature. The densities of the layers are such as to give slight gravitational stability. (The relatively large uncertainties in salinity indicated in Fig. 2A apply only to the region very near the interface; the uncertainties in salinity difference drop to about one-tenth of these values deeper in the mixed layers.) It is interesting that this balance is so close where the salt fingers are observed.

Laboratory shadowgraphs of salt fingers are similar to the images of Fig. 1A. An example of such a photograph is image a of Fig. 1B. To obtain this picture, the optical portion of SCIMP was immersed in a large tank of seawater and the surface of the water was heated with lamps to generate the fingers. The salinity at the surface increased with evaporation, creating conditions favorable for salt fingering. The instrument was then turned on. The profile at the time of exposure is illustrated in Fig. 2B. Salinity samples for this profile were drawn off at three points for subsequent analysis and a thermistor was lowered to five different depths. The appearance of vertical bands in the presence of decreasing temperature and salinity with depth are indicative of laboratory salt fingers. Subsequently, the tank was vigorously stirred and image b of Fig. 1B was taken. The pattern that remains is typical of a photograph where the water is homogeneous; the vertical bands are absent.

When laboratory fingers are viewed from above, they appear square-packed in several well-ordered domains. The domains are aligned randomly over a long path, but some domains are aligned with the rows of descending fingers (high refractive index) parallel to the optic axis. These rows produce the dark bands on the shadowgraph, while the adjacent rows of ascending fingers (low refractive index) produce the light bands. Only these alignments produce a net refractive effect; other alignments are homogeneous when integrated over the ray paths through them, and therefore do not affect the image. The visible rows run at 45° to the cell edges (viewed from above, the fingers are like the squares on a checkerboard, where the rows of one color run at 45° to the edge of the board) so the length of the edge of a cell (the diameter of a single finger) is 0.707 times the separation of the dark bands. Thus, the diameter of fingers was about 6 mm in the Mediterranean outflow interface and about 3.5 mm in the laboratory.

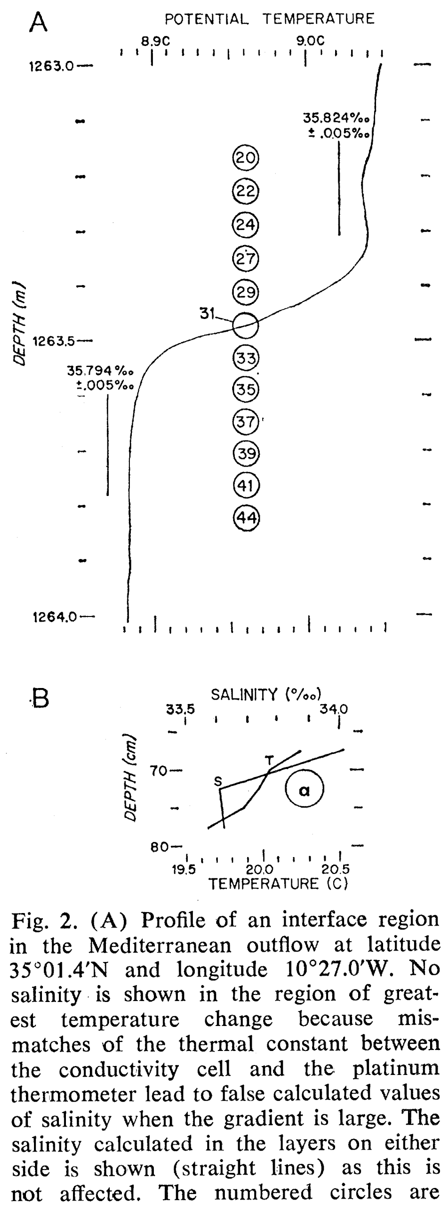

Fig. 2. (A) Profile of an interface region in the Mediterranean outflow at latitude 35°01.4′N and longitude 10°27.0′W. No salinity is shown in the region of greatest temperature change because mismatches of the thermal constant between the conductivity cell and the platinum thermometer lead to false calculated values of salinity when the gradient is large. The salinity calculated in the layers on either side is shown (straight lines) as this is not affected. The numbered circles are the positions of the photographs in Fig. 1A. Potential temperature, the temperature a sample would have if it were raised adiabatically to the ocean surface, has gradients similar to those of the actual temperature over this scale. For information concerning the ocean at lesser and greater depths, see (*8*). (B) Profile of laboratory tank when salt fingers were photographed [reproduced from (*9*)]. Image a in Fig. 1B occupied the region shown by a circle here; *S*, salinity; *T*, temperature.

The dependence of the diameter of a finger on the temperature gradient was derived by Stern (*6*) as

$$a \simeq \frac{\pi}{2}\left|\frac{g\alpha\frac{\partial T}{\partial z}}{4\nu K_T}\right|^{-1/4}$$

where a is the length of a cell edge, $g = 980$ cm/sec^2 is the acceleration of gravity, α is the relative change in density due to temperature for seawater, $\partial T/\partial z$ is the temperature gradient, ν is the kinematic viscosity of seawater, and $K_T = 1.4 \times 10^{-3}$ cm^2/sec is the diffusivity of heat. For the Mediterranean outflow, $\alpha = -1.8 \times 10^{-4}$ °C^{-1}, $\nu = 1.40 \times 10^{-2}$ cm^2/sec, and $\partial T/\partial z = 7.5 \times 10^{-3}$ °C/cm, giving 7.8 mm for a, 30 percent higher than observed. For the laboratory, $\alpha = -2.5 \times 10^{-4}$ °C^{-1}, $\nu = 1.05 \times 10^{-2}$ cm^2/sec, and $\partial T/\partial z = 5.0 \times 10^{-2}$ °C/cm, giving 4.2 mm for a, 20 percent higher than observed. The agreement with theory is acceptable, and the agreement between the two cases is within the uncertainties of the observation.

The observed dimensions of the fingers in the Mediterranean outflow also agree remarkably well with the prediction by Linden (*7*) that the length of fingers in the outflow should be 20 cm and the diameter should be 5 mm. The layers on either side (*8*) are much thinner, however, than the 40 m which he predicted from a calculation of the steady state.

The similarity in appearance of the images in the outflow interface to the images in the laboratory tank, the correlation of vertically banded images with sharp decreases of temperature and salinity with depth, and the agreement in functional dependence of finger size between the natural and controlled cases of fingering, indicate the existence of salt fingers in the ocean.

ALBERT J. WILLIAMS 3RD
Woods Hole Oceanographic Institution, Woods Hole, Massachusetts 02543

References and Notes

1. W. H. Munk, *Deep-Sea Res.* **13**, 707 (1966).
2. J. D. Woods, *J. Fluid. Mech.* **32**, 791 (1967).
3. J. S. Turner, *Deep-Sea Res.* **14**, 599 (1967).
4. M. R. Howe and R. I. Tait, *ibid.* **17**, 963 (1970); R. I. Tait and M. R. Howe, *Nature (Lond.)* **231**, 178 (1971).
5. The observational techniques and the way salt fingers form shadowgraph images are described elsewhere (A. J. Williams 3rd, in preparation).
6. M. E. Stern, *J. Fluid Mech.* **35**, 209 (1969).
7. P. F. Linden, *Deep-Sea Res.* **20**, 325 (1973).
8. The interface region of Fig. 2A occurs beneath a salinity maximum at 1210 m. The temperature and salinity are 9.65°C and 35.90 per mil at 1210 m and 8.65°C and 35.73 per mil at 1310 m. The layer immediately above the interface at 1263.5 m is 2.3 m thick, and the layer below is 1.9 m thick. Each of these layers is terminated by an interface less sharp than the one at 1263.5 m.
9. C. S. Albro, thesis, Woods Hole Oceanographic Institution and Massachusetts Institute of Technology (1972).
10. The autonomous platform "Autoprobe," which carried the instruments, was designed and built by K. H. Burt, the salinity-temperature-depth profiler was designed by N. L. Brown, and I developed the optical instrument; all of the development was done at the Woods Hole Oceanographic Institution. The laboratory tank tests were performed by C. S. Albro. P. J. Hendricks assisted in acquiring the data. I thank Burt, Brown, Albro, and Hendricks for their contributions. The development of the instrumentation was sponsored by ONR contract N00014-66-CO241; NR 083-004, and the study of the Mediterranean outflow was supported by the Oceanography Section of the National Science Foundation, NSF grant GA-37767. This is Contribution No. 3081 from the Woods Hole Oceanographic Institution.

27 December 1973; revised 28 January 1974 ■

Attempt to Date Early South African Hominids by Using Fission Tracks in Calcite

Abstract. *Calcite crystals extracted from marrow cavities of bones found in hominid-bearing breccias from Makapansgat and Swartkrans were studied for fossil tracks. The absence of the expected numbers of tracks in these and in calcites from Beds I and II, Olduvai Gorge, combined with the results of laboratory heating experiments, indicates that track annealing has occurred at ambient temperatures and precludes the widespread use of calcite for fission track dating.*

At the present time there exist no radiometric dates for the early hominid remains from South Africa, so that all attempts to define a time scale for this fossil lineage, and indeed to correlate the various South African sites, have been based on indirect methods such as analysis of faunal assemblages or, more recently, on geomorphological studies [for an excellent recent review of age estimates for the South African hominids see (*1*)]. In view of the importance of correct age determinations for reconstructing the evolution of the early hominids and for intermeshing the South African fossils with those from East Africa, we have attempted to date by fission tracks samples from two of the South African cave sites, Makapansgat and Swartkrans. The indirect dating methods suggest ages of ~ 3 and ~ 2 million years, respectively, for the hominid remains from these sites (*1*).

All of the South African hominid remains occur in limestone deposits, and in many cases the bone marrow cavities are lined with large, clear calcite crystals (Fig. 1a) which presumably grew relatively soon after the bones themselves were deposited. On the basis of an earlier report (*2*) that fission track dating of calcite is feasible, such crystals seemed ideal because (i) they have remained since their deposition in a protected cave environment and therefore should never have experienced temperatures high enough to erase fission tracks, and (ii) the size and optically clear quality of the crystals are optimal for fission tract studies The South African samples analyzed were numerous crystals from marrow cavities in bones from the red, pink, and gray (hominid-rich) breccias at Makapansgat and crystals from the travertine overlying the orange breccia at Swartkrans. In addition we have studied calcite crystals from Beds I and II, Olduvai Gorge (*3*).

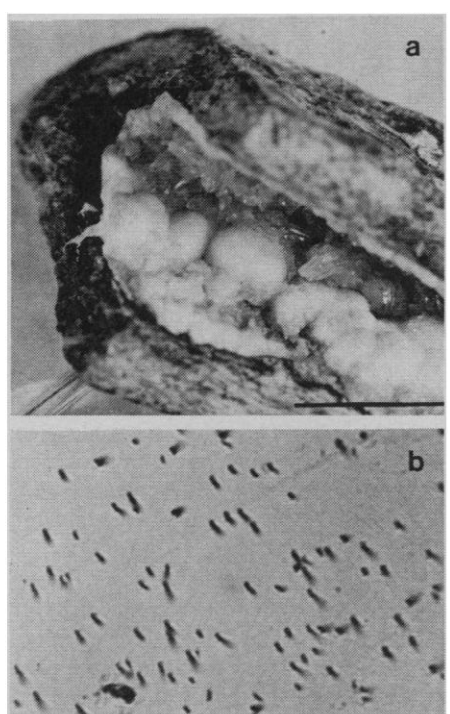

Fig. 1. (a) Milky botryoidal and clear euhedral calcite in marrow cavity of a bone from the hominid-rich gray breccia at Makapansgat. Scale bar, 1 cm. (b) Californium-252 fission tracks in one of the clear euhedral crystals shown in (a). The tracks were etched by using the solution described in the text. Scale bar, 20 μm.

The solutions used by Sippel and Glover (*2*) to etch fission tracks in calcite produce rectangular pits similar to dislocation etch pits rather than the more desirable linear tracks with small cone angles that are produced in other minerals under proper etching conditions. Thus, our initial experiments revolved around an attempt to develop a better etching solution for calcite. The most satisfactory etchant that emerged, one which produces beautiful narrow tracks with small cone angles (Fig. 1b), is the olivine etch described by Krishnaswami *et al.* (*4*), with NaOH added to *p*H 12 (*5*). Other etchants that we found to be almost as satisfactory are 2*M* NaOH, the olivine etch (*4*) without added NaOH, or a saturated solution of disodium ethylenediaminetetraacetate mixed with an equal volume of 5 percent acetic acid.

The uranium concentrations of the various calcites are given in Table 1. These values were determined by using the induced fission track method (*6*) for individual calcite crystals. Except for the travertine sample from Swartkrans, where considerable variation from crystal to crystal was observed, the uranium content measured in different crystals from the same sample or from the same bone marrow cavity is quite constant. The variation from sample to sample, however, is more than two orders of magnitude. The most logical explanation for this large variation is difference in uranium concentration of the groundwater from which the calcite precipitated, although if this is the case the difference between 64-7-7A and 70-6-29M from Bed II, Olduvai Gorge, is difficult to explain. There are no obvious geological differences between these two lacustrine beds (*7*). For one chip of pink breccia from Makapansgat, a section was made through an embedded bone fragment and the distribution of uranium was studied in the section as a whole. The calcite crystals projecting